Materials Advances

rsc.li/materials-advances

ROYAL SOCIETY
OF **CHEMISTRY**

COMMUNICATION
Benoît H. Lessard *et al.*
Synthetically facile organic solar cells with >4% efficiency
using P3HT and a silicon phthalocyanine non-fullerene
acceptor

Check for updates

Synthetically facile organic solar cells with >4% efficiency using P3HT and a silicon phthalocyanine non-fullerene acceptor†

Trevor M. Grant,[a] Chloé Dindault,[a] Nicole A. Rice,[a] Sufal Swaraj [b] and Benoît H. Lessard [ID] *[ac]

We demonstrate organic photovoltaic devices with extremely low synthetic complexity by pairing poly(3-hexithiophene) (P3HT) with a novel non-fullerene acceptor (NFA) bis(tri-*n*-propylsilyl oxide) silicon phthalocyanine ((3PS)$_2$-SiPc). (3PS)$_2$-SiPc possesses a relatively unique combination of high solubility and excellent thermal stability, facilitating its ease of processing by both solution and sublimation techniques. Binary P3HT/(3PS)$_2$-SiPc devices achieved an average power conversion efficiency of 4.3%, a new record for SiPc NFAs. AFM and synchrotron STXM measurements reveal a unique morphology of P3HT/(3PS)$_2$-SiPc, with significant phase separation due to the strong crystallization of (3PS)$_2$-SiPc.

Rapid progress in solution-processed organic photovoltaic (OPV) devices over the last five years has come largely from the development of novel non-fullerene acceptors (NFAs). In combination with low bandgap polymer donors, record power conversion efficiencies (PCEs) above 18% have been achieved.[1] However, in the pursuit of maximizing PCE, the scale-up feasibility of many novel NFAs has not been considered in their design leading to increasingly complex molecules. It has become apparent that the synthetic complexity of NFAs and polymer donors must be reduced for the realization of commercial OPV devices.[2] This understanding has prompted increased research interest in the design of less complex NFAs to pair with poly-(3-hexithiophene) (P3HT), which continues to be the most scalable and cost effective polymer donor. PCEs as high as 9% have been achieved in P3HT/NFA devices, however the synthetic complexity of the incorporated NFAs remains prohibitively high.[3,4]

Derivatives of phthalocyanine are appealing materials for synthetically simple active materials in OPV devices given their established scale-up chemistry for use as dyes and pigments and known efficacy in organic electronic devices.[5] Silicon phthalocyanine (SiPc) derivatives prepared from straightforward synthetic routes have been established as effective ternary additives in solution-processed OPV devices,[6–8] and have shown potential for use as NFAs.[9,10] In recent work, we demonstrated that using alkylsiloxy-functionalized SiPc as an NFA with P3HT can yield devices with a promising PCE of 3.6%, slightly higher than a PCE of 3.4% achieved when combined with the state-of-the-art polymer poly[(2,6-(4,8-bis(5-(2-ethylhexyl)thiophen-2-yl)-benzo[1,2-*b*:4,5-*b*′]dithiophene))-*alt*-(5,5-(1′,3′-di-2-thienyl-5′,7′-bis(2-ethylhexyl)benzo[1′,2′-*c*:4′,5′-*c*′]dithiophene-4,8-dione)] (PBDB-T).[11] The synthetic simplicity of SiPc derivatives compels continuing investigations into its use as an NFA, specifically paired with P3HT to minimize the overall synthetic complexity of the active layer materials. In this work, we show that the SiPc derivative bis(tri-*n*-propylsilyl oxide) silicon phthalocyanine ((3PS)$_2$-SiPc), which possesses a unique combination of excellent solubility and thermal properties, can achieve an impressive PCE of 4.3% as an NFA in a P3HT-based device.

The chemical synthesis of (3PS)$_2$-SiPc is outlined in the ESI† (Scheme S1). The conjugated macrocycle of SiPc is formed in a 1-step reaction of diiminoisoindoline with silicon tetrachloride to form silicon phthalocyanine dichloride. The substitution of tripropylsiloxy ligands can then be performed in a 1-step reaction with tripropylchlorosilane in the presence of sodium hydroxide and a phase transfer catalyst.[12] This straightforward synthetic pathway is in contrast to many high-performance NFAs in the literature, such as Y6 which requires 15 steps to synthesize from commercial reagents.[13]

The chemical structure, energy levels, and optical absorption of (3PS)$_2$-SiPc in relation to P3HT and PC$_{61}$BM are shown in Fig. 1. A maximum absorption of 672 nm was measured in toluene solution, with a corresponding molar extinction coefficient of 4.2×10^5 M^{-1} cm^{-1}. HOMO and LUMO energy levels of 5.3 eV

[a] Department of Chemical and Biological Engineering, University of Ottawa, 161 Louis Pasteur, Ottawa, ON, K1N 6N5, Canada

[b] SOLEIL Synchrotron, L'Orme des Merisiers, Saint-Aubin, P. O. Box 48, CEDEX, FR-91192 Gif-Sur-Yvette, France

[c] School of Electrical Engineering and Computer Science, University of Ottawa, 800 King Edward Ave., Ottawa, ON, K1N 6N5, Canada.
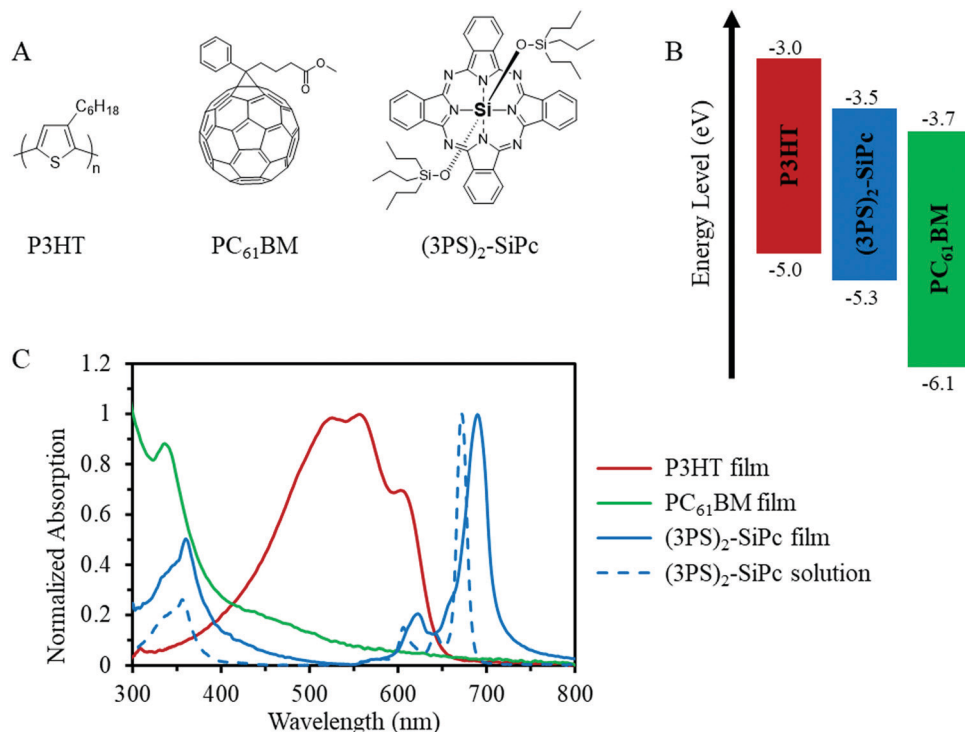*E-mail: benoit.lessard@uottawa.ca*

Fig. 1 (A) Chemical structures, (B) energy levels, and (C) UV-Vis absorption of thin films of P3HT, PC$_{61}$BM and (3PS)$_2$-SiPc, as well as (3PS)$_2$-SiPc in toluene.

and 3.5 eV, respectively, were estimated from cyclic voltammetry measurements (Fig. S2, ESI†) and the optical band gap. (3PS)$_2$-SiPc also exhibited a strong tendency to crystalize from solution, easily producing large crystals grown from chloroform solvent evaporation. The observed optoelectrical properties and high crystallinity are typical for SiPc derivatives with alkylsiloxy functional groups.[14]

Our group has recently reported the synthesis and characterization of a series of soluble alkylsiloxy-functionalized SiPcs with a range of chain lengths.[15] Naturally, ligands with shorter alkyl chains provide lower solubility to the planar conjugated phthalocyanine macrocycle. In this work, we have found that tri-*n*-propylsiloxy ligands are the shortest chain length that can be incorporated while still providing sufficient solubility ($>$15 mg mL^{-1}) for effective processing as an NFA from chlorinated solvents. SiPc derivatives functionalized with bulkier triisopropylsiloxy or shorter triethylsiloxy ligands yield maximum concentrations below 10 mg mL^{-1} in 1,2-dichlorobenzene, rendering them impractical for use as NFAs.

Interestingly, in addition to strong solubility, (3PS)$_2$-SiPc readily sublimes at 200 °C under 100 mTorr pressure, significantly lower than its decomposition temperature at approximately 340 °C measured by thermogravimetric analysis (Fig. S3, ESI†). Differential scanning calorimetry measurements also show that (3PS)$_2$-SiPc has no phase transitions between 25 °C and 240 °C, allowing it to directly sublime upon heating (Fig. S4, ESI†). This is in contrast to previously reported SiPc derivatives with longer tributylsiloxy or trihexylsiloxy ligands which have a melting transition below their sublimation temperature and therefore undergo distillation

instead of sublimation.[10] The ability for a soluble organic compound to sublime is highly advantageous, given sublimation purification is relatively simple to perform on larger kilogram scales. This obviates the need to employ resource intensive solution-based purification techniques such as column chromatography, reducing time and materials costs during synthesis. To highlight the processability of (3PS)$_2$-SiPc, we fabricated planar heterojunction (PHJ) devices processed by physical vapor deposition (PVD) paired with alpha-sexithiophene (α-6T) as a small molecule donor. The PHJ α-6T/(3PS)$_2$-SiPc devices show relatively low performance with an average PCE of 0.73 $\pm$ 0.06%, short circuit current density (J_{SC}) of 2.2 $\pm$ 0.1 mA cm^{-2}, open circuit voltage (V_{OC}) of 0.62 $\pm$ 0.01 V, and fill factor (FF) of 0.53 $\pm$ 0.03 (Fig. S5, ESI†). These device metrics are comparable to previously reported PHJ devices utilizing fluorophenoxy-functionalized SiPcs paired with α-6T.[16] The α-6T/(3PS)$_2$-SiPc devices were not characterized further due to their relatively poor performance, however they readily demonstrate the ability of (3PS)$_2$-SiPc to be processed by sublimation (Fig. S5, ESI†).

The performance of (3PS)$_2$-SiPc as an NFA with P3HT was evaluated in inverted bulk heterojunction (BHJ) OPV devices (glass/ITO/ZnO/active layer/MoO$_x$/Ag) with an active area of 0.325 cm^2. Current density–voltage (J–V) characteristics for optimized devices at 1 sun AM 1.5G are shown in Fig. 2A, and tabulated device metrics in Table 1. Baseline P3HT/PC$_{61}$BM devices fabricated for comparison yielded an average PCE of 3.0 $\pm$ 0.1%, consistent with average performance reported in the literature.[17] P3HT/(3PS)$_2$-SiPc devices were optimized to a thickness of approximately 100 nm, with performance found to be dependant
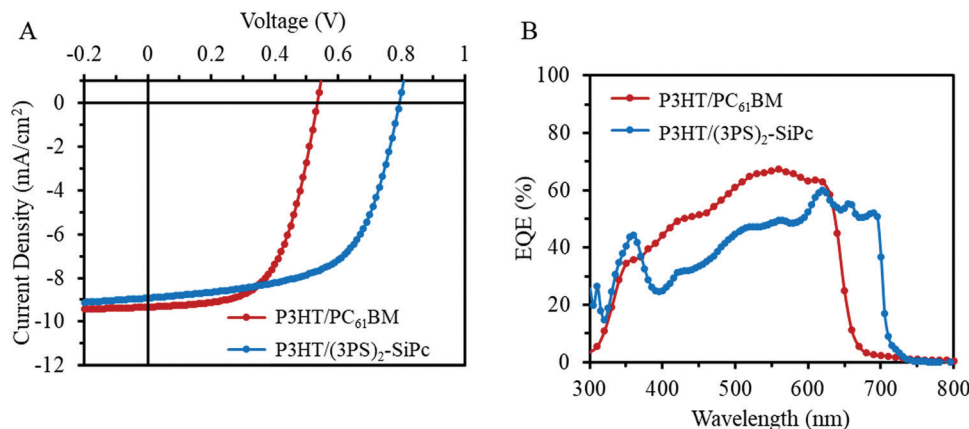
Fig. 2 (A) Characteristic current density–voltage (J–V) curves measured under 1000 W m^{-2} AM1.5G irradiation and (B) their respective EQE spectra.

on the molecular weight of P3HT. Maximum PCE was achieved using a moderately low P3HT molecular weight of 35 kDa, consistent with results reported for other NFAs in the literature.[18] Interestingly, annealing did not increase the PCE for devices prepared using this low molecular weight P3HT, with maximum efficiency observed for as cast devices. Optimized devices achieved an average PCE of 4.3 ± 0.2%, with a J_{SC} of 8.9 ± 0.5 mA cm^{-2}, V_{OC} of 0.79 ± 0.01 V, and FF of 0.61 ± 0.01. These values are the highest reported for an OPV device employing a SiPc derivative. The device metrics are similar to the PC$_{61}$BM baseline devices, except for a greater V_{OC} of approximately 0.8 V due to the more favorable shallow LUMO level of (3PS)$_2$-SiPc (Fig. 1B). External quantum efficiency (EQE) is shown in Fig. 2B. P3HT/(3PS)$_2$-SiPc devices show a weaker contribution from P3HT absorption below 600 nm compared to the baseline P3HT/PC$_{61}$BM devices, however the increased spectral coverage from the strong phthalocyanine contribution between 680 nm and 700 nm affords a comparable J_{SC}.

It is important to note that while SiPc derivatives have conventionally been used as an additive in ternary devices, the average PCE of 4.3% herein reported for binary P3HT/SiPc devices surpasses the PCE achieved in ternary P3HT/PC$_{61}$BM/SiPc devices. For comparison, ternary P3HT/PC$_{61}$BM/(3PS)$_2$-SiPc devices show an average PCE of 3.4 ± 0.1%, J_{SC} of 10.4 ± 0.2 mA cm^{-2}, V_{OC} of 0.55 ± 0.02 V, and FF of 0.59 ± 0.02 (Fig. S6, ESI†), consistent with similar alkylsiloxy SiPc derivatives.[15] The addition of (3PS)$_2$-SiPc as a ternary additive effectively provides a J_{SC} increase of 12% compared to P3HT/PC$_{61}$BM devices, while its use as an NFA in place of PC$_{61}$BM results in a V_{OC} increase of approximately 50% affording a significantly higher PCE. This demonstrates that appropriately designed SiPc derivatives may be more suitable for use as NFAs when paired with P3HT, eliminating the requirement

to include PC$_{61}$BM to achieve a competitive PCE and dramatically reducing the combined synthetic complexity active materials.

The morphology of P3HT/(3PS)$_2$-SiPc and P3HT/PC$_{61}$BM films were compared using atomic force microscopy (AFM) shown in Fig. 3. The P3HT/PC$_{61}$BM film was relatively smooth with an RMS roughness of 9.5 nm. The film surface consists of fine-grained features on the nanoscale, indicating a well mixed donor/acceptor network. The P3HT/(3PS)$_2$-SiPc film was significantly rougher with a film surface dominated by larger crystalline features, yielding an RMS roughness of 15.7 nm. These large domains are generally unfavorable for achieving efficient exciton dissociation, with optimal P3HT/NFA systems characterized by domain sizes on the order of 10–20 nm.[3,4] The highly crystalline nature of (3PS)$_2$-SiPc is likely the cause of the relatively large domain sizes.

The blend film morphologies were further characterized by scanning transmission X-ray microscopy (STXM), with the resulting through-plane composition maps shown in Fig. 4. The composition maps of P3HT/PC$_{61}$BM and P3HT/(3PS)$_2$-SiPc blended films were drawn from thickness values obtained from singular value decomposition (SVD) of energy stacks at the carbon K-edge using absorption spectra of reference films for each of the active materials (P3HT, PC$_{61}$BM, and (3PS)$_2$-SiPc) (Fig. S7, ESI†).[19–21] Experimental optical density (OD) spectra of reference films were scaled down to an elemental thickness of 1 nm using simulated OD spectra. These 1 nm experimental OD spectra were used to fit energy stacks of the different blends following the SVD linear regression using the software aXis2000.[29] For P3HT/acceptor blended films, the 1 nm experimental spectra of the pure reference films were used for the SVD fitting to yield thickness maps of both components of the blend. The composition maps shown in Fig. 4 are obtained from

Table 1 Current density–voltage characteristics of BHJ OPV devices measured at AM1.5G 1000 W m^{-2}

Active layer	PCE^a [%]	J_{SC} (J–V)^a [mA cm^{-2}]	J_{SC} (EQE) (mA cm^{-2})	$V_{OC}{}^a$ [V]	FF^a
P3HT/PC$_{61}$BM	3.0 ± 0.1	9.3 ± 0.1	9.7	0.53 ± 0.01	0.60 ± 0.01
P3HT/(3PS)$_2$-SiPc	4.3 ± 0.2	8.9 ± 0.5	9.6	0.79 ± 0.01	0.61 ± 0.01

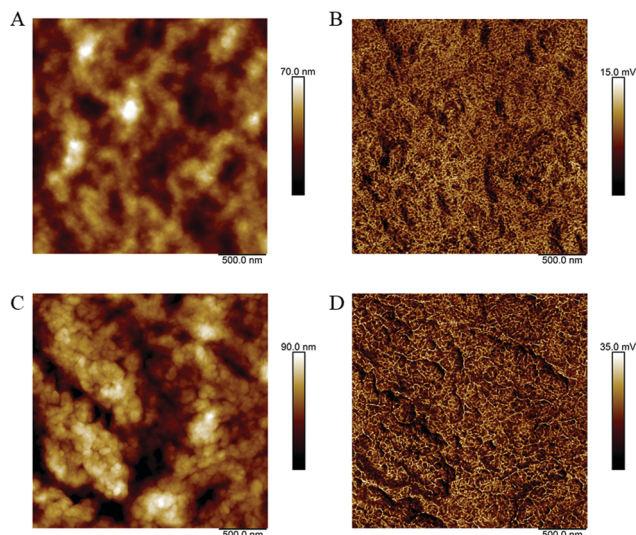^{a} Average and standard deviation for at least 10 devices.

Fig. 3 AFM (A) height and (B) inphase images for P3HT/PC$_{61}$BM films, as well as (C) height and (D) inphase images for P3HT/(3PS)$_2$-SiPc.

Table 2 Synthetic complexity (SC) for (3PS)$_2$-SiPc in relation to PC$_{61}$BM and commonly used high performance NFAs

Acceptor	NSS	RY	NUO	NCC	NHC	SC[a]	Ref.
(3PS)$_2$-SiPc	2	3.9	1	0	4	12	This work
PC$_{61}$BM	5	23.2	6	2	6	32	26
O-IDTBR	11	23.1	24	6	16	55	26
A1	7	3.5	16	5	29	37	26
ITIC-2F	13	44.5	22	8	30	66	27
ITIC	10	142	19	8	28	67	27
Y6	15	8.9	28	6	25	59	28

[a] To maintain consistency with the literature, the values used for normalization are: NSS$_{max}$ = 22, RY$_{max}$ = 86.9, NUO$_{max}$ = 39, NCC$_{max}$ = 13, NHC$_{max}$ = 44.

the thickness maps as follows: % of P3HT = thickness of P3HT/ (thickness of P3HT + thickness of acceptor).

For both blended films, the composition maps show similar characteristics to the surface topographies obtained from AFM. The P3HT/PC$_{61}$BM film shows a relatively small variance in composition with no distinct features, indicative of a homogeneous morphology. The measured compositions are consistent with a 1 : 1 weight ratio P3HT/PC$_{61}$BM blended film having a molar ratio of approximately 0.84 : 0.16 (P3HT : PC$_{61}$BM). The P3HT/(3PS)$_2$-SiPc composition maps indicate large domains rich with (3PS)$_2$-SiPc on the same scale as the topographic features observed in AFM images. This further suggests that the large topographic features

are comprised of mainly (3PS)$_2$-SiPc arising from crystallization during film formation. It is possible through suppression of SiPc crystallization and reduced domain sizes that the exciton dissociation efficiency could be improved to afford increased J_{SC} and FF values, further justifying the continued interest into these promising NFAs. The long term thermal and morphological stability of binary P3HT/SiPc devices also remains to be investigated.

To highlight the chemical simplicity and scale-up potential of (3PS)$_2$-SiPc we evaluated its relative synthetic complexity index (SC) in relation to PC$_{61}$BM and several NFAs commonly employed for achieving high PCE devices in the literature, shown in Table 2. The SC was defined using the model introduced by Po *et al.* (eqn (1)), which has become a standard for comparing the relative scalability and cost of active materials in OPV devices.[22] The model uses five weighted parameters to define the SC: the number of synthetic steps (NSS), the reciprocal of the cumulative synthetic yield (RY), the number of unit operations (NUO), the number of column chromatography purification steps (NCC), and the number of highly hazardous chemicals
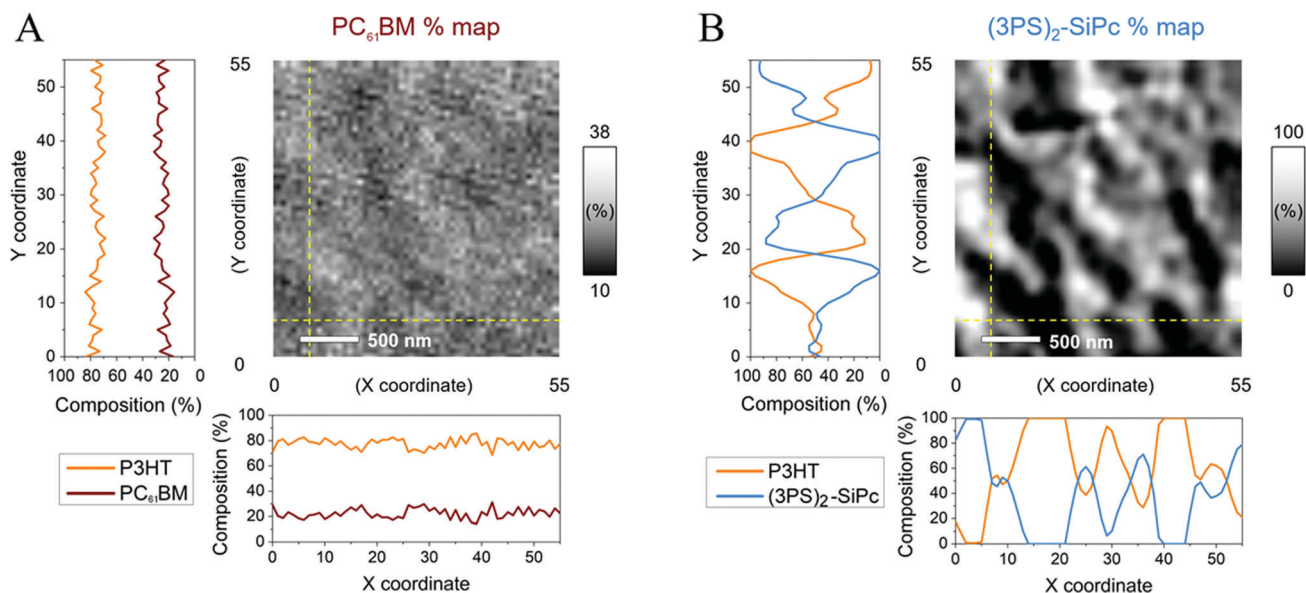

Fig. 4 Percentage composition maps of (A) PC$_{61}$BM in P3HT/PC$_{61}$BM blend and (B) (3PS)$_2$-SiPc in P3HT/(3PS)$_2$-SiPc blend obtained from singular value decomposition of STXM energy stacks. Profile lines Y = 7 and X = 7 are plotted for each blend.

involved in the synthesis (NHC). Each parameter is normalized to the maximum value within the group of materials being compared.

$$SC = 35\frac{NSS}{NSS_{max}} + 25\frac{\log(RY)}{\log(RY_{max})} + 15\frac{NUO}{NUO_{max}} + 15\frac{NCC}{NCC_{max}} + 10\frac{NHC}{NHC_{max}} \quad (1)$$

A relative SC index of 12 was calculated for $(3PS)_2$-SiPc, lower than any of the other NFAs surveyed by a factor of three. The extremely low SC index of $(3PS)_2$-SiPc results from a combined effect of a two-step synthesis from commercially available starting materials, circumvention of the use of highly hazardous chemicals such as *n*-butyllithium or organotin compounds, and the ability to be purified exclusively by sublimation thus eliminating column chromatography steps. Notably, the SC for $(3PS)_2$-SiPc is approximately 4.5 times lower than that of O-IDTBR, which is currently the leading candidate NFA for the upscaling of P3HT-based devices.[23–25] The SC is also approximately three times lower than A1, a recently shown simplified analogue of O-IDTBR.[26] The extremely low SC of $(3PS)_2$-SiPc, combined with a competitive PCE above 4% in P3HT-based devices, demonstrates excellent promise for phthalocyanines as low cost NFAs.

In summary, we have shown a novel silicon phthalocyanine derivative $(3PS)_2$-SiPc with the rare ability to be processed by both PVD and solution techniques. Solution processed P3HT/$(3PS)_2$-SiPc BHJ OPV devices achieved a high average PCE of 4.3%, the highest reported value for binary or ternary blends of P3HT with SiPcs. AFM and STXM measurements reveal the $(3PS)_2$-SiPc forms relatively large domains due to its highly crystalline nature. Future work suppressing the crystallization of $(3PS)_2$-SiPc may yield a more optimal morphology to increase J_{SC} and FF. These promising results pave the way for inexpensive solar energy generation using a polymer donor and NFA that are synthetically facile to synthesize on a commercial scale.

Conflicts of interest

There are no conflicts to declare.

Acknowledgements

References

1 Q. Liu, Y. Jiang, K. Jin, J. Qin, J. Xu, W. Li, J. Xiong, J. Liu, Z. Xiao, K. Sun, S. Yang, X. Zhang and L. Ding, 18% Efficiency Organic Solar Cells, *Sci. Bull.*, 2020, **65**(4), 272–275.

2 A. Wadsworth, M. Moser, A. Marks, M. S. Little, N. Gasparini, C. J. Brabec, D. Baran and I. McCulloch, Critical Review of the Molecular Design Progress in Non-Fullerene Electron Acceptors towards Commercially Viable Organic Solar Cells, *Chem. Soc. Rev.*, 2019, **48**(6), 1596–1625.

3 X. Xu, G. Zhang, L. Yu, R. Li and Q. Peng, P3HT-Based Polymer Solar Cells with 8.25% Efficiency Enabled by a Matched Molecular Acceptor and Smart Green-Solvent Processing Technology, *Adv. Mater.*, 2019, **31**, 1906045.

4 C. Yang, S. Zhang, J. Ren, M. Gao, P. Bi, L. Ye, J. Hou, S. Zhang, L. Ye and J. Hou, Molecular Design of a Non-Fullerene Acceptor Enables a P3HT-Based Organic Solar Cell with 9.46% Efficiency, *Energy Environ. Sci.*, 2020, **13**(9), 2864–2869.

5 C. G. Claessens, U. Hahn and T. Torres, Phthalocyanines: From Outstanding Electronic Properties to Emerging Applications, *Chem. Rec.*, 2008, **8**(2), 75–97.

6 S. Honda, T. Nogami, H. Ohkita, H. Benten and S. Ito, Improvement of the Light-Harvesting Efficiency in Polymer/Fullerene Bulk Heterojunction Solar Cells by Interfacial Dye Modification, *ACS Appl. Mater. Interfaces*, 2009, **1**(4), 804–810.

7 T. M. Grant, T. Gorisse, O. Dautel, G. Wantz and B. H. Lessard, Multifunctional Ternary Additive in Bulk Heterojunction OPV: Increased Device Performance and Stability, *J. Mater. Chem. A*, 2017, **5**(4), 1581–1587.

8 L. Ke, J. Min, M. Adam, N. Gasparini, Y. Hou, J. D. Perea, W. Chen, H. Zhang, S. Fladischer, A. C. Sale, E. Spiecker, R. R. Tykwinski, C. J. Brabec and T. Ameri, A Series of Pyrene-Substituted Silicon Phthalocyanines as Near-IR Sensitizers in Organic Ternary Solar Cells, *Adv. Energy Mater.*, 2016, **6**(7), 1502355.

9 E. Zysman-Colman, S. S. Ghosh, G. Xie, S. Varghese, M. Chowdhury, N. Sharma, D. B. Cordes, A. M. Z. Slawin and I. D. W. Samuel, Solution-Processable Silicon Phthalocyanines in Electroluminescent and Photovoltaic Devices, *ACS Appl. Mater. Interfaces*, 2016, **8**(14), 9247–9253.

10 M. T. Dang, T. M. Grant, H. Yan, D. S. Seferos, B. H. Lessard and T. P. Bender, Bis(Tri-n-Alkylsilyl Oxide) Silicon Phthalocyanines: A Start to Establishing a Structure Property Relationship as Both Ternary Additives and Non-Fullerene Electron Acceptors in Bulk Heterojunction Organic Photovoltaic Devices, *J. Mater. Chem. A*, 2017, **5**(24), 12168–12182.

11 T. M. Grant, K. L. C. Kaller, T. J. Coathup, N. A. Rice, K. Hinzer and B. H. Lessard, High Voc Solution-Processed Organic Solar Cells Containing Silicon Phthalocyanine as a Non-Fullerene Electron Acceptor, *Org. Electron.*, 2020, **87**, 105976.

12 T. Gessner; R. Sens; W. Ahlers and C. Vamvakaris, Preparation of Silicon Phthalocyanines and Germanium Phthalocyanines and Related Substances, *US Pat.*, US 2010/0113767 A1, 2010.

13 J. Yuan, Y. Zhang, L. Zhou, G. Zhang, H. L. Yip, T. K. Lau, X. Lu, C. Zhu, H. Peng, P. A. Johnson, M. Leclerc, Y. Cao, J. Ulanski, Y. Li and Y. Zou, Single-Junction Organic Solar Cell with over 15% Efficiency Using Fused-Ring Acceptor with Electron-Deficient Core, *Joule*, 2019, **3**(4), 1140–1151.

14 B. H. Lessard, J. D. Dang, T. M. Grant, D. Gao, D. S. Seferos and T. P. Bender, Bis(Tri-n-Hexylsilyl Oxide) Silicon Phthalocyanine: A Unique Additive in Ternary Bulk Heterojunction Organic Photovoltaic Devices, *ACS Appl. Mater. Interfaces*, 2014, **6**, 15040–15051.

15 M. C. Vebber, T. M. Grant, J. L. Brusso and B. H. Lessard, Bis(Trialkylsilyl Oxide) Silicon Phthalocyanines: Understanding the Role of Solubility in Device Performance as Ternary Additives in Organic Photovoltaics, *Langmuir*, 2020, **36**(10), 2612–2621.

16 B. H. B. H. Lessard, T. M. Grant, R. White, E. Thibau, Z.-H. Lu and T. P. Bender, The Position and Frequency of Fluorine Atoms Changes the Electron Donor/Acceptor Properties of Fluorophenoxy Silicon Phthalocyanines within Organic Photovoltaic Devices, *J. Mater. Chem. A*, 2015, **3**, 24512–24524.

17 M. T. Dang, L. Hirsch and G. Wantz, P3HT:PCBM, Best Seller in Polymer Photovoltaic Research, *Adv. Mater.*, 2011, **23**(31), 3597–3602.

18 A. Wadsworth, Z. Hamid, M. Bidwell, R. S. Ashraf, J. I. Khan, D. H. Anjum, C. Cendra, J. Yan, E. Rezasoltani, A. A. Y. Guilbert, M. Azzouzi, N. Gasparini, J. H. Bannock, D. Baran, H. Wu, J. C. de Mello, C. J. Brabec, A. Salleo, J. Nelson, F. Laquai and I. McCulloch, Progress in Poly (3-Hexylthiophene) Organic Solar Cells and the Influence of Its Molecular Weight on Device Performance, *Adv. Energy Mater.*, 2018, **8**(28), 1801001.

19 I. N. Koprinarov, A. P. Hitchcock, C. T. McCrory and R. F. Childs, Quantitative Mapping of Structured Polymeric Systems Using Singular Value Decomposition Analysis of Soft X-Ray Images, *J. Phys. Chem. B*, 2002, **106**(21), 5358–5364.

20 J. Kinyangi, D. Solomon, B. Liang, M. Lerotic, S. Wirick and J. Lehmann, Nanoscale Biogeocomplexity of the Organomineral Assemblage in Soil, *Soil Sci. Soc. Am. J.*, 2006, **70**(5), 1708–1718.

21 A. Michelin, E. Drouet, E. Foy, J. J. Dynes, D. Neff and P. Dillmann, Investigation at the Nanometre Scale on the Corrosion Mechanisms of Archaeological Ferrous Artefacts by STXM, *J. Anal. At. Spectrom.*, 2013, **28**(1), 59–66.

22 R. Po, G. Bianchi, C. Carbonera and A. Pellegrino, "All That Glisters Is Not Gold": An Analysis of the Synthetic Complexity of Efficient Polymer Donors for Polymer Solar Cells, *Macromolecules*, 2015, 453–461.

23 S. Holliday, R. S. Ashraf, A. Wadsworth, D. Baran, S. A. Yousaf, C. B. Nielsen, C. H. Tan, S. D. Dimitrov, Z. Shang, N. Gasparini, M. Alamoudi, F. Laquai, C. J. Brabec, A. Salleo, J. R. Durrant, I. Mcculloch and M. Alamoudi, High-Efficiency and Air-Stable P3HT-Based Polymer Solar Cells with a New Non-Fullerene Acceptor, *Nat. Commun.*, 2016, **7**, 11585.

24 D. Corzo, K. Almasabi, E. Bihar, S. Macphee, D. Rosas-Villalva, N. Gasparini, S. Inal and D. Baran, Digital Inkjet Printing of High-Efficiency Large-Area Nonfullerene Organic Solar Cells, *Adv. Mater. Technol.*, 2019, **4**(7), 1900040.

25 M. Fernández Castro, E. Mazzolini, R. R. Sondergaard, M. Espindola-Rodriguez and J. W. Andreasen, Flexible ITO-Free Roll-Processed Large-Area Nonfullerene Organic Solar Cells Based on P3HT:O-IDTBR, *Phys. Rev. Appl.*, 2020, **14**(3), 034067.

26 T. R. Andersen, A. T. Weyhe, Q. Tao, F. Zhao, R. Qin, S. Zhang, H. Chen and D. Yu, Novel Cost-Effective Acceptor:P3HT Based Organic Solar Cells Exhibiting the Highest Ever Reported Industrial Readiness Factor, *Mater. Adv.*, 2020, **1**(4), 658–665.

27 X. Du, T. Heumueller, W. Gruber, A. Classen, T. Unruh, N. Li and C. J. Brabec, Efficient Polymer Solar Cells Based on Non-Fullerene Acceptors with Potential Device Lifetime Approaching 10 Years, *Joule*, 2019, **3**(1), 215–226.

28 C. J. Brabec, A. Distler, X. Du, H. J. Egelhaaf, J. Hauch, T. Heumueller and N. Li, Material Strategies to Accelerate OPV Technology Toward a GW Technology, *Adv. Energy Mater.*, 2020, **10**(43), 2001864.

29 aXis2000, available online: http://unicorn.mcmaster.ca/aXis2000.html.